

## Local and Remote Charge-Transfer-Enhanced Raman Scattering on One-Dimensional Transition-Metal Oxides

Bin Dong,<sup>[a, b]</sup> Yingzhou Huang,<sup>[a]</sup> Naisen Yu,<sup>[b]</sup> Yurui Fang,<sup>[a]</sup> Baosheng Cao,<sup>[b]</sup> Yuanzuo Li,<sup>[a, c]</sup> Hongxing Xu,<sup>[a, d]</sup> and Mengtao Sun<sup>\*[a]</sup>

**Abstract:** The one-dimensional (1D) transition-metal oxide MoO<sub>3</sub> belt is synthesized and characterized with X-ray diffraction, scanning electron microscopy, and Raman spectroscopy. Charge-transfer-(CT) enhanced Raman scattering of 4-mercaptobenzoic acid (4-MBA) on a 1D MoO<sub>3</sub> belt was investigated experimentally and theoretically. The chemical enhancement of

surface-enhanced Raman scattering (SERS) of 4-MBA on the MoO<sub>3</sub> belt by CT is in the order of 10<sup>3</sup>. The SERS of 4-MBA was investigated theoretically by using a quantum chemical

**Keywords:** charge transfer · raman scattering · transition metals · X-ray diffraction

method. The remote SERS of 4-MBA along the 1D MoO<sub>3</sub> belt (the light excitation to one side of the MoO<sub>3</sub> belt, and the SERS spectrum is collected on the other side of the MoO<sub>3</sub> belt) is also shown experimentally, which provides potential applications of SERS. The incident polarization dependence of remote SERS spectra has also been investigated experimentally.

### Introduction

Surface-enhanced Raman scattering (SERS) has attracted much attention in different fields, such as electrochemistry, surface science, catalysis, and chemical and biomolecular sensing because of its extremely high surface sensitivity and powerful application for fingerprint vibrational spectroscopy in qualitative and quantitative analysis.<sup>[1,2]</sup> Before the mid-

1990s, most investigation focused on the three “coinage metals” (Au, Ag, and Cu) as they can provide a large enhancement through surface plasmon resonance (SPR).<sup>[3,4]</sup> Since the mid-1990s, SERS for different transition metals has been investigated gradually because of the importance of transition metals (VIII B group elements) in electrochemistry and catalysis.<sup>[5]</sup> Recently, Sun et al.<sup>[6]</sup> and Musumeci et al.<sup>[7]</sup> observed the enhanced Raman scattering for molecules adsorbed on metallic oxides (TiO<sub>2</sub> and ZnO) nanoparticles. They observed nanoparticle size-dependent SERS and interpreted them as a chemical-enhancement mechanism or charge-transfer (CT) mechanism. Until now, SERS on the one-dimensional (1D) belt of transition-metal oxides has not been reported and the enhancement mechanism is not clear. Among transition-metal oxides, MoO<sub>3</sub> has many distinctive properties and was used in electronic display systems, gas sensors, catalysts, and also in other applications. Also, MoO<sub>3</sub> can be developed for 1D objects, the most-frequent being ribbon-shaped belts of micrometer or nanometer diameters.<sup>[8]</sup> Remote SERS has been investigated by utilizing propagation SPR along an Ag nanowire,<sup>[9]</sup> which has not previously been reported along a 1D belt of transition-metal oxides. It is important to determine the mechanism of local and remote SERS on a 1D belt of transition-metal oxides.

Herein, we experimentally report on the SERS of 4-mercaptobenzoic acid (4-MBA; see Figure 1a) adsorbed on a 1D MoO<sub>3</sub> belt and theoretically interpret the enhancement

[a] Prof. B. Dong, Dr. Y. Huang, Dr. Y. Fang, Dr. Y. Li, Prof. H. Xu, Prof. M. Sun  
Beijing National Laboratory for Condensed Matter Physics  
Institute of Physics  
Chinese Academy of Sciences  
P. O. Box 603-146, Beijing, 100190 (P.R. China)  
Fax: (+86)10-8264-8147  
E-mail: mtsun@aphy.iphy.ac.cn

[b] Prof. B. Dong, Dr. N. Yu, Dr. B. Cao  
School of Science  
Dalian Nationalities University  
Dalian, 116600 (P.R. China)

[c] Dr. Y. Li  
School of Physics and Optoelectronic Technology  
Dalian University of Technology  
Dalian 116024 (P.R. China)

[d] Prof. H. Xu  
Division of Solid State Physics  
Lund University  
Lund 22100 (Sweden)

Supporting information for this article is available on the WWW under <http://dx.doi.org/10.1002/asia.200900706>.

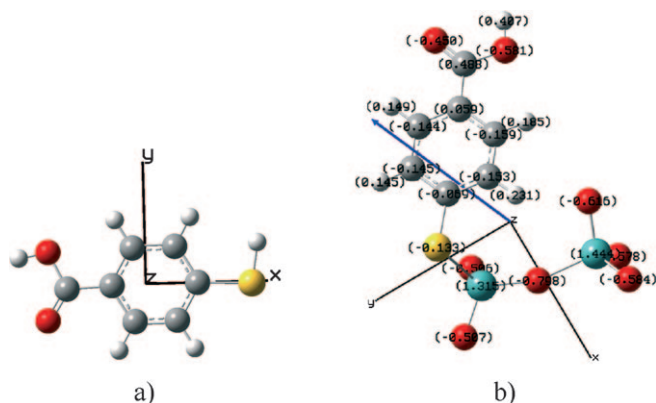


Figure 1. a) 4-MBA-(MoO<sub>3</sub>)<sub>2</sub> and b) 4-MBA-(MoO<sub>3</sub>)<sub>2</sub> complex in which the Cartesian coordinate was shown. These results were further used in Table 1.

mechanism with CT between molecular and transition-metal oxides. Theoretically, SERS of 4-MBA was investigated by using a quantum chemical method. Utilizing the propagation of the light along the 1D MoO<sub>3</sub> belt, the remote SERS (light excited at one side of the MoO<sub>3</sub> belt, and SERS signal is collected on the other side of the MoO<sub>3</sub> belt) is also reported experimentally. The incident polarization dependence of remote SERS spectra has also been investigated experimentally.

## Results and Discussion

Figure 2a shows the XRD pattern of the MoO<sub>3</sub> belts, which indicates that the belts consist of phase  $\alpha$ -MoO<sub>3</sub>. The diffraction peaks of the XRD pattern for the MoO<sub>3</sub> belts can be readily indexed to be orthorhombic with lattice constants of  $a=3.962$  Å,  $b=13.855$  Å,  $c=3.701$  Å (JCPDS no. 89-5108). Observation of only (0/0) lines in the diffraction pattern of the as-grown belts reveals that the thickest portion of the belt is along the  $b$  axis. Figure 2b,c show the morphology investigations, which were characterized with SEM. The width range of the MoO<sub>3</sub> belts is from 0.3 to 3 μm and the maximum length is about 80 μm. The surface of the MoO<sub>3</sub> belts is clean, flat, and has no obvious defects. The EDS (inset of Figure 2b) indicated the abundance of oxygen owing to the average O/Mo ratio of 3.3, which is higher than the stoichiometric ratio 3. The Raman spectroscopy of the MoO<sub>3</sub> belts at an incident light wavelength of 632.8 nm was measured (see Figure 2d. It was found that all Raman peaks of MoO<sub>3</sub> belts are below 1000 cm<sup>-1</sup>. The SERS spectra of 4-MBA on MoO<sub>3</sub> belts was not influenced by the Raman peaks of MoO<sub>3</sub> in the region 1050–1700 cm<sup>-1</sup>.

Figure 3a shows the experimental SERS spectrum of 4-MBA adsorbed on the MoO<sub>3</sub> belts from 10<sup>-3</sup> M ethanol solution and the normal Raman spectra of 4-MBA with 0.1 M ethanol solution. It is clearly shown that the Raman signals of 4-MBA adsorbed on the MoO<sub>3</sub> belts are remarkably in-

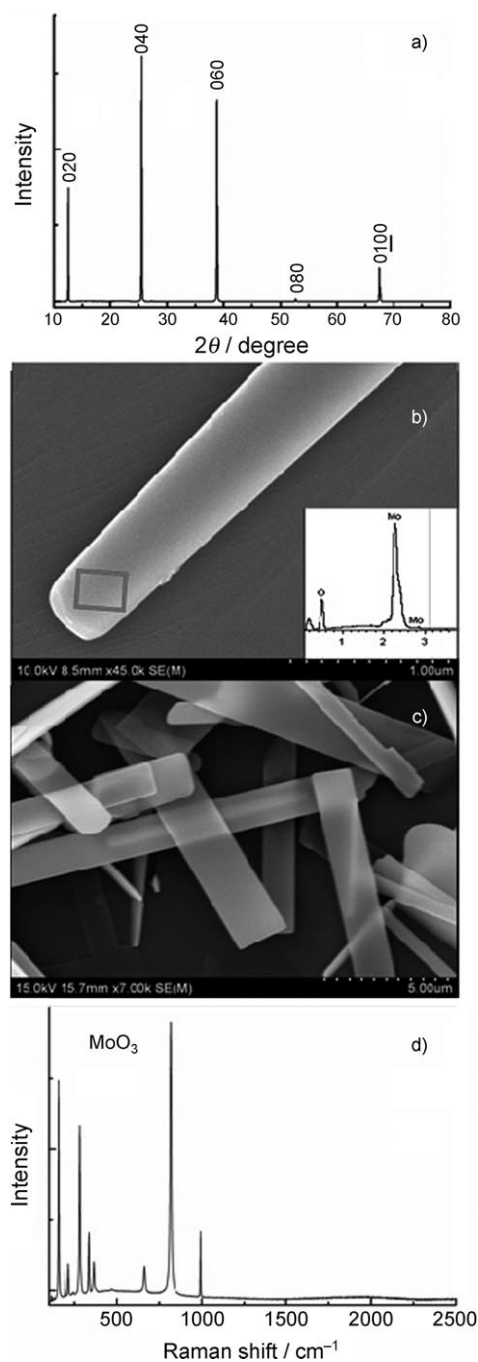


Figure 2. a) The XRD of the MoO<sub>3</sub> belts, b) and c) the SEM images of the MoO<sub>3</sub> belts, and d) Raman spectrum of the MoO<sub>3</sub> belts. The inset in Figure 2b is the EDS.

creased relative to the 4-MBA in solution. The simulated SERS spectrum of 4-MBA can be seen in Figure 3b. It was found that the simulated SERS spectrum of 4-MBA can well reproduce experimental spectra. The SERS spectra of 4-MBA and 4-MBA adsorbed on the MoO<sub>3</sub> belts are similar and dominated by the strong bands at about 1096 cm<sup>-1</sup> and 1594 cm<sup>-1</sup>, which are assigned to aromatic-ring vibrations that possess the C–S stretching characteristics and aromatic-

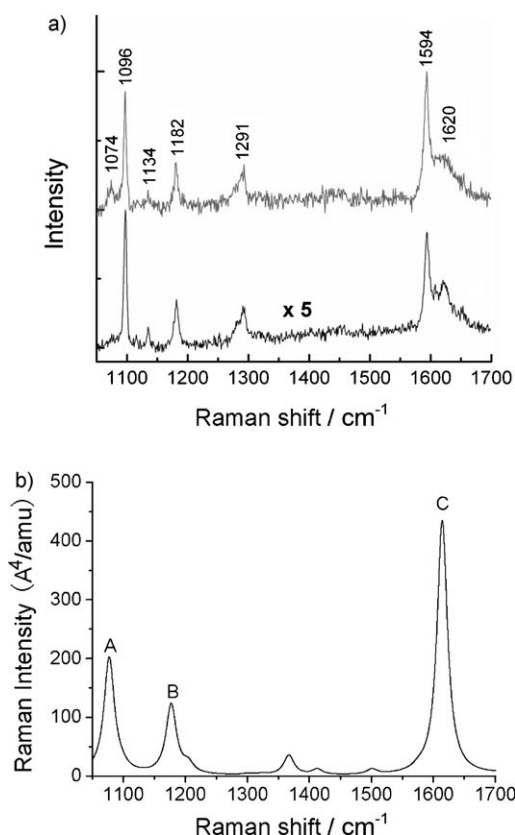


Figure 3. a) the SERS spectrum (top) of 4-MBA adsorbed on the MoO<sub>3</sub> belts from 10<sup>-3</sup>M ethanol solution and the normal Raman spectrum (bottom) of 4-MBA with 0.1 M ethanol solution. The integral time is 10 seconds and laser power is 0.5 mW in SERS. b) the simulated SERS spectrum of 4-MBA in which the vibrational frequencies were scaled by 0.98. Note, A, B, and C refer to vibrational modes described in Figure 4.

ring vibration. The weak band at 1620 cm<sup>-1</sup> is C=O stretching mode. Other weak bands at about 1134 cm<sup>-1</sup> (ν<sub>15</sub>, b<sub>2</sub>) and 1182 cm<sup>-1</sup> (ν<sub>15</sub>, b<sub>2</sub>) corresponding to the C-H deformation modes were also observed. The weak band at 1291 cm<sup>-1</sup> is the δCH+νCC mode. Three normal modes of strong peaks (A, B, and C) in Figure 3b can also be seen in Figure 4.

There are two kinds of enhancement mechanisms, that is, chemical and electromagnetic enhancement mechanisms,

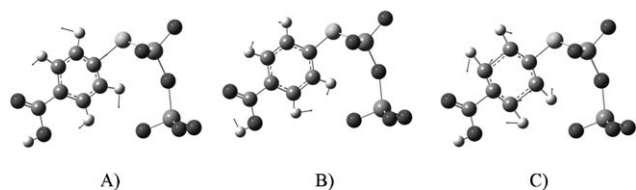


Figure 4. Three vibrational modes (A, B, and C) from Figure 3b.

which are relative and show change of polarizability and local electromagnetic enhancement, respectively (Equation (1)).

$$I = \left| \frac{\partial \alpha}{\partial Q_0} \right|^2 \left| \frac{E_{loc}}{E_0} \right|^4 \quad (1)$$

In Equation (1), α is the polarizability, Q<sub>0</sub> is the shift of normal mode, E<sub>loc</sub> is the local electromagnetic field, and E<sub>0</sub> is the incident light. To study the chemical enhancement mechanism of SERS, we studied the ground-state properties of the 4-MBA-(MoO<sub>3</sub>)<sub>2</sub> complex. The optimized geometry of the 4-MBA-(MoO<sub>3</sub>)<sub>2</sub> complex can be seen in Figure 1b, in which the angle of C-S-Mo in the 4-MBA-(MoO<sub>3</sub>)<sub>2</sub> complex is 101.7°. This indicates that the dihedral angle between 4-MBA and the MoO<sub>3</sub> belt is 101.7° (the 4-MBA does not stand perpendicular to the surface of the MoO<sub>3</sub> belt). The atom-resolved Mulliken charge distribution can be seen in Figure 1b as well as a 0.83 electron transfer from 4-MBA to (MoO<sub>3</sub>)<sub>2</sub> in which Mulliken charges with hydrogen atoms are summed into heavy atoms. CT results show increases in the static dipole moment (the orientation of static dipole moment can be seen in Figure 1b) and static polarizability (see data in Table 1). The increased polarizability then results in the chemical enhancement of SERS via CT. To check if there is resonance enhancement on SERS of 4-MBA, we calculated electronic transitions of the 4-MBA-(MoO<sub>3</sub>)<sub>2</sub> complex. From Table 2, we found that there was no electronic transitions for the 4-MBA-(MoO<sub>3</sub>)<sub>2</sub> complex when the wavelength was larger than 327 nm as the lowest singlet electronic transition for the 4-MBA-(MoO<sub>3</sub>)<sub>2</sub> complex is at 327 nm. In our experimental SERS measurement, the wavelength of the laser was 632.8 nm. As a result, there is no resonant effect on the SERS of 4-MBA adsorbed on the MoO<sub>3</sub> belt. From Table 2, the electronic transitions for the 4-MBA-(MoO<sub>3</sub>)<sub>2</sub> complex are within the ultraviolet region. We also studied the properties of electronic transi-

Table 1. The static dipole moment (Debye) static electronic polarizability in which the Cartesian coordinate of them can be seen from Figure 1.

	Static dipole moment			Static electronic polarizability		
	x	y	z	xx	yy	zz
4-MBA	0.8292	2.2295	0.0005	156	94	36
4-MBA-(MoO <sub>3</sub> ) <sub>2</sub> complex	-7.1438	3.0240	-1.0526	264	209	126

Table 2. Singlet-singlet electronic transitions of 4-MBA-(MoO<sub>3</sub>)<sub>2</sub> complex.

	Energy [nm]	f
S <sub>1</sub>	327.17	0.0562
S <sub>2</sub>	314.70	0.0008
S <sub>3</sub>	307.18	0.0589
S <sub>4</sub>	301.11	0.0009
S <sub>5</sub>	298.74	0.0076
S <sub>6</sub>	287.28	0.0055

tions with charge-difference density,<sup>[16]</sup> the results of which can be seen in Figure 5. It was found that  $S_1$  and  $S_3$  are CT excited states; whereas the other four excited states are localized excited states in which the hole and electron are localized on  $(\text{MoO}_3)_2$ .

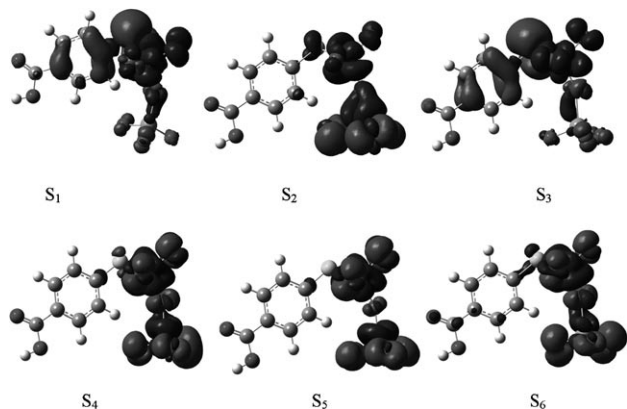


Figure 5. Charge difference densities of 4-MBA- $(\text{MoO}_3)_2$  complex for the lowest six singlet excited states in which the green and red stand for hole and electron, respectively.

Utilizing the properties of light propagating along 1D  $\text{MoO}_3$ , the remote SERS (light excited at one side of the  $\text{MoO}_3$  belt, and SERS is collected on the other side of the  $\text{MoO}_3$  belt, see Figure 6a, b) is also reported experimentally. From Figure 6b, the light can efficiently propagate along the 1D  $\text{MoO}_3$  belt from point A to point C with strong light (the length of this belt is about  $52 \mu\text{m}$ ). The SERS collection is at point B, which is located about  $12.6 \mu\text{m}$  away from the left-end side of the  $\text{MoO}_3$  belt (point A). For the local SERS, the light and collection occurs at point B, while for remote SERS, the collection of SERS is at point B, and the excited light at the left-end side of  $\text{MoO}_3$  belt (point A). Figure 6c shows the results of measurement of local and remote SERS spectra. It can be seen that remote SERS can also be clearly observed when the light propagates about  $12.6 \mu\text{m}$  along the  $\text{MoO}_3$  belt. The intensity of remote SERS is decreased to  $1/200$ , compared with local SERS.

The incident polarization dependence of remote SERS spectra has also been investigated experimentally. From Figure 7, it was found that there is no polarization dependence on remote SERS of 4-MBA. Compared with the length of the  $\text{MoO}_3$  belt, the width of the  $\text{MoO}_3$  belt is small, so this belt can be considered as a 1D belt. Whereas the width of this  $\text{MoO}_3$  belt is about  $3 \mu\text{m}$ , compared with the incident light of  $632.8 \text{ nm}$ , the  $\text{MoO}_3$  belt can be considered as a two-dimensional belt. Therefore, polarization dependence on remote SERS of 4-MBA cannot be observed experimentally.

We attempted to estimate the SERS enhanced factor (EF) by using Equation (2).

$$EF = (I_{\text{SERS}}/N_{\text{SERS}})/(I_{\text{NR}}/N_{\text{NR}}) \quad (2)$$

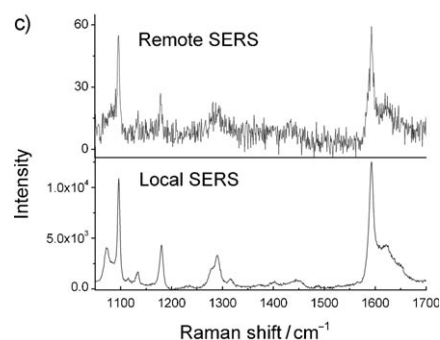
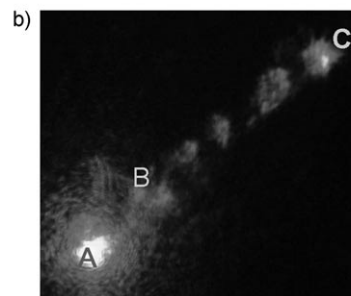
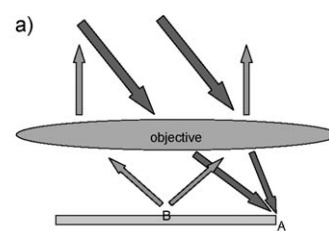


Figure 6. a) The diagram of remote SERS, b) the propagation of light along  $\text{MoO}_3$  belt in which the distance between point A and B is about  $12.6 \mu\text{m}$ , and the length of this belt is about  $52 \mu\text{m}$ , and c) the local and remote SERS spectrum of 4-MBA adsorbed on the  $\text{MoO}_3$  belts from  $10^{-3} \text{ M}$  ethanol solution. The integral time is 30 seconds and laser power is  $5 \text{ mW}$  in SERS.

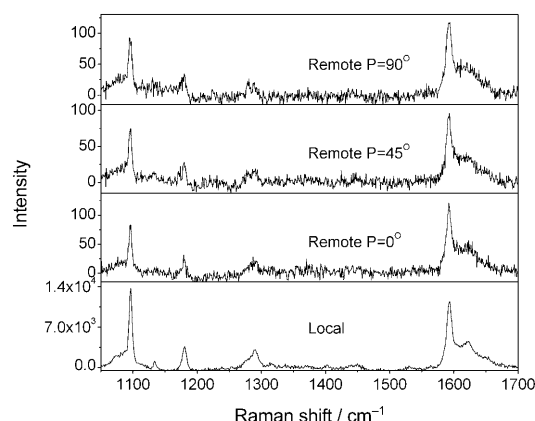


Figure 7. The incident polarization (P) dependence of remote SERS spectra.

In Equation (2),  $I_{\text{SERS}}$  denotes the SERS intensity of the  $1594 \text{ cm}^{-1}$  ( $\nu_{8a}$ ) band of 4-MBA adsorbed on the  $\text{MoO}_3$  belt by using  $632.8 \text{ nm}$  radiation as the excitation source,  $I_{\text{NR}}$  de-

notes the normal Raman (NR) scattering intensity of the same band of 4-MBA, and  $N_{\text{SERS}}$  and  $N_{\text{NR}}$  are the numbers of 4-MBA molecules effectively excited by the laser beam to obtain the corresponding SERS and NR spectra, respectively. After centrifugation and rinse, the molecules form a monolayer on the  $\text{MoO}_3$  belt. As the molecules almost lay on the surface of  $\text{MoO}_3$  belt (discussed above), the effective area of the detected single molecule is about  $S_{\text{m}} = 0.65 \text{ nm}^2$ . The effective area of laser spot is about  $S_{\text{L}} = 2 \text{ }\mu\text{m}^2$ , so the number of detected molecule on  $\text{MoO}_3$  belt can therefore be summarized by Equation (3).

$$N_{\text{SERS}} = 2 \times 10^{-12} \text{ m}^2 / (0.65 \times 10^{-18} \text{ m}^2) \approx 3 \times 10^6 \quad (3)$$

The effective detection volume of the Raman spectroscopic system is approximately  $V_{\text{D}} = S_{\text{L}} \times H = 2 \text{ }\mu\text{m}^2 \times 5 \text{ }\mu\text{m} = 10 \text{ }\mu\text{m}^3$ , where  $H$  is effective detection depth. The number of molecules in the effective detection volume in solution is therefore described in Equation (4).

$$N_{\text{NR}} = 6 \times 10^{23} / \text{M} \times 10^{-1} (\text{M L}^{-1}) \times V_{\text{D}} \approx 6 \times 10^8 \quad (4)$$

Considering the  $I_{\text{SERS}}/I_{\text{NR}} = 5$  in Figure 3a, we determined that the  $EF$  is in the order of  $10^3$ , which is in accord with Equation (2).

## Conclusions

1D transition-metal oxide  $\text{MoO}_3$  belt was synthesized and characterized with X-ray diffraction, scanning electron microscopy, and Raman spectroscopy. SERS of 4-MBA on the 1D  $\text{MoO}_3$  belt were observed experimentally, and the enhancement mechanism was interpreted theoretically with CT. The chemical enhancement of SERS on the 1D  $\text{MoO}_3$  belt can reach up to  $10^3$ . The remote SERS of 4-MBA along the 1D  $\text{MoO}_3$  belt has been realized experimentally. There is no polarization dependence on remote SERS of 4-MBA along 1D  $\text{MoO}_3$  belt with the width of  $3 \text{ }\mu\text{m}$ . These findings significantly extend the applications of SERS.

## Experimental Section

The  $\text{MoO}_3$  belts were prepared by a vapor transport method.  $(\text{NH}_4)_6\text{Mo}_7\text{O}_{24} \cdot 4\text{H}_2\text{O}$  (10 g) was placed in an  $\text{Al}_2\text{O}_3$  crucible and heated to the sintering temperature of 1523 K with a heating rate of  $5^\circ\text{C min}^{-1}$ , maintained for 1 h. The gap between the door and the furnace was enlarged to have a 3–4 mm free space for easy airflow, and  $\text{MoO}_3$  belts that are white and transparent grow in a certain region at 600–800 K near the door of the furnace. Structural and phase-purity characterizations were carried out by powder X-ray diffraction (XRD) by using a SHIMADZU XRD-6000 diffractometer with  $\text{Cu}_{\text{K}\alpha}$  radiation. The morphology investigations were characterized by scanning electron microscopy (SEM) with energy dispersive spectroscopy (EDS; Hitachi S-4800).

$\text{MoO}_3$  belts that were surface modified by molecules were obtained as follows:  $\text{MoO}_3$  belts (5 mg) were dissolved in 10 ml of 4-mercaptobenzoic acid (4-MBA;  $1 \times 10^{-3} \text{ M}$ ) ethanol solution, and the mixture was stirred for 2 h. The precipitate was centrifuged and rinsed with purified water once more. Then, the  $\text{MoO}_3$  belts that were modified by 4-MBA were ob-

tained. Raman spectra were measured with a confocal Raman spectroscopic system (Renishaw 2000, Invia) through an objective  $50\times$  lens with a numerical aperture (NA) of 0.75. The 632.8-nm radiation from the He-Ne laser was used as an excitation source. The Raman spectral resolution was  $0.8 \text{ cm}^{-1}$ . The incident polarization dependence of remote SERS spectra has also been investigated experimentally. For comparison, the Raman spectrum of  $\text{MoO}_3$  belts is also measured at the incident light of 632.8 nm. All measurements were carried out at room temperature.

## Theoretical Methods

To interpret the enhancement mechanism of SERS, the ground-state geometry of the 4-MBA-( $\text{MoO}_3$ )<sub>2</sub> complex (Figure 1b) was optimized with density functional theory (DFT)<sup>[10]</sup>, B3LYP functional,<sup>[11]</sup> as well as the 6-31G(D) basis set for O, S, C, H, and the LanL2DZ basis set<sup>[12]</sup> for Mo. With the optimized ground-state geometry, the Raman spectrum was calculated at the same level of theory. To check if there was resonance enhancement on SERS of 4-MBA, electronic transitions of the 4-MBA-( $\text{MoO}_3$ )<sub>2</sub> complex were calculated with time-dependent DFT (TD-DFT),<sup>[13]</sup> the CAM-B3LYP functional<sup>[14]</sup> and 6-31G(D) basis set for O, S, C, H, and LanL2DZ basis set for Mo. For comparison, the ground-state properties of isolated 4-MBA were studied with a DFT, B3LYP functional, and 6-31G(D) basis set. All the quantum chemical calculations were done with Gaussian 09 software.<sup>[15]</sup>

## Acknowledgements

This work was supported by the National Natural Science Foundation of China (Grant Nos. 10874234, 20703064, 90923003 and 10804015), the National Basic Research Project of China (Grant Nos. 2009CB930701, and 2007CB936804), and China Postdoctoral Science Foundation (20090450620).

- [1] M. Moskovits, *Rev. Mod. Phys.* **1985**, *57*, 783.
- [2] K. Kneipp, H. Kneipp, I. Itzkan, R. R. Dasari, M. S. Feld, *Chem. Rev.* **1999**, *99*, 2957.
- [3] H. X. Xu, E. J. Bjerneld, M. Kail, L. Borjesson, *Phys. Rev. Lett.* **1999**, *83*, 4357.
- [4] J. R. Lombardi, R. L. Birke, *J. Phys. Chem. C* **2008**, *112*, 5605.
- [5] Z. Q. Tian, B. Ren, *Annu. Rev. Phys. Chem.* **2004**, *55*, 197.
- [6] Z. H. Sun, B. Zhao, J. R. Lombardi, *Appl. Phys. Lett.* **2007**, *91*, 221106.
- [7] A. Musumeci, D. Gosztola, T. Schiller, N. M. Dimitrijevic, V. Mujica, D. Martin, T. Rajh, *J. Am. Chem. Soc.* **2009**, *131*, 6040.
- [8] L. Q. Mai, B. Hu, W. Chen, Y. Y. Qi, C. S. Lao, R. S. Yang, Y. Dai, Z. L. Wang, *Adv. Mater.* **2007**, *19*, 3712.
- [9] Y. R. Fang, H. Wei, F. Hao, P. Nordlander, H. X. Xu, *Nano Lett.* **2009**, *9*, 2049.
- [10] P. Hohenberg, W. Kohn, *Phys. Rev.* **1964**, *136*, B864.
- [11] a) A. D. Becke, *J. Chem. Phys.* **98**, **1993**, 5648; b) C. Lee, W. Yang, R. G. Parr, *Phys. Rev. B* **1988**, *37*, 785.
- [12] P. J. Hay, W. R. Wadt, *J. Chem. Phys.* **1985**, *82*, 270.
- [13] R. Bauernschmitt, R. Ahlrichs, *Chem. Phys. Lett.* **1996**, *256*, 454.
- [14] T. Yanai, D. Tew, N. Handy, *Chem. Phys. Lett.* **2004**, *393*, 51.
- [15] *Gaussian 09*, Revision B.02, M. J. Frisch, G. W. Trucks, H. B. Schlegel, G. E. Scuseria, M. A. Robb, J. R. Cheeseman, G. Scalmani, V. Barone, B. Mennucci, G. A. Petersson, H. Nakatsuji, M. Caricato, X. Li, H. P. Hratchian, A. F. Izmaylov, J. Bloino, G. Zheng, J. L. Sonnenberg, M. Hada, M. Ehara, K. Toyota, R. Fukuda, J. Hasegawa, M. Ishida, T. Nakajima, Y. Honda, O. Kitao, H. Nakai, T. Vreven, J. A. Montgomery, Jr., J. E. Peralta, F. Ogliaro, M. Bearpark, J. J. Heyd, E. Brothers, K. N. Kudin, V. N. Staroverov, R. Kobayashi, J. Normand, K. Raghavachari, A. Rendell, J. C. Burant, S. S. Iyengar, J. Tomasi, M. Cossi, N. Rega, J. M. Millam, M. Klene, J. E. Knox, J. B. Cross, V. Bakken, C. Adamo, J. Jaramillo, R. Gomperts, R. E. Stratmann, O. Yazyev, A. J. Austin, R. Cammi, C. Pomelli, J. W.

Ochterski, R. L. Martin, K. Morokuma, V. G. Zakrzewski, G. A. Voth, P. Salvador, J. J. Dannenberg, S. Dapprich, A. D. Daniels, O. Farkas, J. B. Foresman, J. V. Ortiz, J. Cioslowski, and D. J. Fox, Gaussian Inc., Wallingford CT, **2009**.

[16] M. T. Sun, S. S. Liu, M. D. Chen, H. X. Xu, *J. Raman Spectrosc.* **2009**, *40*, 137.

Received: December 10, 2009

Revised: March 25, 2010

Published online: June 10, 2010